J. Chem. Eng. Data **2006,** *51,* 2145−2155

Temperature and Composition Dependence of the Density and Viscosity of Binary Mixtures of Water + Ionic Liquid

Héctor Rodríguez[†] and Joan F. Brennecke*

Department of Chemical and Biomolecular Engineering, University of Notre Dame, Notre Dame, Indiana 46556

Density and viscosity were determined for binary mixtures of water and three ionic liquids: 1-ethyl-3-methylimidazolium ethylsulfate, 1-ethyl-3-methylimidazolium trifluoroacetate, and 1-ethyl-3-methylimidazolium trifluoromethanesulfonate. The experimental measurements of these properties were carried out at atmospheric pressure and temperatures from (278.15 to 348.15) K. The temperature dependence of density and viscosity for these systems can be described by an empirical second-order polynomial and by the Vogel−Fulcher−Tammann equation, respectively. Excess molar volumes and viscosity deviations were calculated and correlated by Redlich−Kister polynomial expansions. The latter correlations describe the variation of density and viscosity with composition. Comparison of the results for the three binary systems elucidates the influence of the anion on these physical properties.

Introduction

The term ionic liquid (IL) has come to define, in recent years, a family of substances entirely constituted by ions with melting points below 373 K.[1,2] A wide variety of ILs remain liquid at room temperature and even at temperatures well below that. Among their unique characteristics,[2,3] the ability to solubilize an enormous variety of compounds, a negligible vapor pressure under common process conditions, a wide liquid range, and the possibility to tailor their chemical structure at will to better match a given target are particularly noteworthy. This interesting set of properties has spurred the increasing attention drawn to ILs by both industry and academia over the past decade. While applications of ILs in a diverse range of fields, such as electrochemistry, separation processes, synthesis, and catalysis, have begun to be explored, much research must be done to fully exploit these interesting fluids.

A major impetus for IL research is the possibility of using them as substitutes for classical industrial solvents, most of which are volatile organic compounds (VOCs).[1] This replacement would lead to a critical reduction in the emission of VOCs to the atmosphere, currently a major source of pollution. Four common strategies to avoid the use of conventional organic solvents are solventless processes, water, supercritical fluids (especially CO_2), and ILs. Combinations of these options may also be considered as environmentally favorable. In our research group, for instance, we have investigated the use of ILs/supercritical CO_2 biphasic systems.[4−7]

Similarly, processes that currently involve homogeneous mixtures of water and a VOC solvent might be improved by substitution of the VOC solvent with a hydrophilic IL. It has been shown, for instance, that water can dramatically decrease the viscosity of ILs, even when only present in small amounts.[8] Thus, a mixture of water and a water-miscible IL might provide an attractive low viscosity alternative to some organic solvents.

The knowledge of thermophysical properties of binary mixtures of water plus hydrophilic ILs is needed for the development of practical applications and design of processes using water + IL systems. To date, a number of papers have studied fundamental properties such as density or viscosity of these binary systems: some of them report values for dilute aqueous solutions of ILs[9−11] or, in the other extreme, the effect of water content in “pure” ILs or binary mixtures with low fractions of water;[8,12−15] whereas only some other works have performed measurements covering the whole composition range.[16−22] Most of the papers in the latter group, however, focus on ILs with either a halide or tetrafluoroborate as the anion, which may lead to corrosion problems or to generation of HF by decomposition.[23] An exception is the work of Yang and coworkers,[10,19] which focused on the density of the binary system water and 1-ethyl-3-methylimidazolium ethylsulfate ([emim][$EtSO_4$]).[24]

In this work, accurate data at atmospheric pressure are reported for the density and viscosity of mixtures of water and three different ILs: [emim][$EtSO_4$], 1-ethyl-3-methylimidazolium trifluoroacetate ([emim][TFA]), and 1-ethyl-3-methylimidazolium trifluoromethanesulfonate ([emim][OTf]) at temperatures from (278.15 to 348.15) K. The temperature dependence of both properties is analyzed and correlated. Excess molar volume and viscosity deviation, calculated from the experimental data, are also correlated and used to characterize the influence of the composition of the mixture on its density and viscosity.

Experimental Section

Chemicals. Two samples of [emim][$EtSO_4$], with a nominal purity greater than 98 %, were purchased from Solvent Innovation; their water content, found to be (23 and 45) ppm, was measured by Karl Fischer titration with a Metrohm 831 KF Coulometer.

Ethyltrifluoromethanesulfonate (Aldrich, 99 %) and 1-methylimidazole (Aldrich, 99 %, freshly redistilled over KOH) were reacted at low temperature in a stirred round-bottomed flask with a reflux condenser in the absence of any solvent to form [emim][OTf]. A similar procedure can be found in the literature.[25] Unreacted starting materials were removed by heating under reduced pressure. The structure of the final product was

---

* Corresponding author. Telephone: (574)631-5847. Fax: (574)631-8366. E-mail: jfb@nd.edu.

[†] Permanent address: Department of Chemical Engineering, University of Santiago de Compostela, E-15782 Santiago de Compostela, Spain.

10.1021/je0602824 CCC: $33.50

Table 1. Experimental Density ρ, Excess Molar Volume V^E, Dynamic Viscosity η, and Viscosity Deviation $\Delta\eta$ for the Binary System Water (1) + [emim][EtSO$_4$] (2)

	T/K							
x_1	278.15	288.15	298.15	308.15	318.15	328.15	338.15	348.15
				ρ/g·cm^{-3}				
0.0000	1.25112	1.24413	1.23737	1.23061	1.22390	1.21723	1.21060	1.20401
0.2112	1.24659	1.23979	1.23299	1.22621	1.21945	1.21274	1.20605	1.19940
0.4119	1.23956	1.23270	1.22585	1.21902	1.21221	1.20541	1.19863	1.19191
0.5939	1.22774	1.22080	1.21387	1.20692	1.19997	1.19301	1.18603	1.17905
0.7669	1.20183	1.19485	1.18781	1.18072	1.17356	1.16634	1.15905	1.15168
0.8487	1.17563	1.16883	1.16192	1.15490	1.14777	1.14052	1.13314	1.12570
0.9292	1.12063	1.11502	1.10914	1.10300	1.09659	1.08992	1.08300	1.07583
0.9683	1.06686	1.06325	1.05904	1.05427	1.04901	1.04329	1.03715	1.03061
0.9916	1.02113	1.01946	1.01678	1.01326	1.00903	1.00416	0.99872	0.99276
1.0000	0.99999	0.99913	0.99707	0.99406	0.99023	0.98571	0.98056	0.97484
				V^E/cm^3·mol^{-1}				
0.0000	0.000	0.000	0.000	0.000	0.000	0.000	0.000	0.000
0.2112	−0.211	−0.215	−0.195	−0.181	−0.166	−0.156	−0.144	−0.136
0.4119	−0.399	−0.372	−0.334	−0.304	−0.278	−0.253	−0.231	−0.215
0.5939	−0.524	−0.470	−0.415	−0.367	−0.325	−0.285	−0.248	−0.213
0.7669	−0.514	−0.439	−0.367	−0.306	−0.249	−0.196	−0.146	−0.097
0.8487	−0.450	−0.371	−0.300	−0.238	−0.182	−0.130	−0.081	−0.037
0.9292	−0.246	−0.185	−0.134	−0.091	−0.054	−0.019	0.012	0.043
0.9683	−0.058	−0.028	−0.003	0.017	0.034	0.050	0.065	0.079
0.9916	−0.013	−0.005	0.001	0.005	0.009	0.013	0.017	0.020
1.0000	0.000	0.000	0.000	0.000	0.000	0.000	0.000	0.000
				η/mPa·s				
0.0000	308	166	95	62	41	30	21	17
0.2245	150	86	54	36	26	19	15	12
0.4084	83	49	33	23	17	13	11	9
0.5976	45	27	19	14	11	9	7	6
0.7675	22	14	10	8	6	6	5	4
0.9292	6	5	4	4	3	3	3	2
				$\Delta\eta$/mPa·s				
0.0000	0	0	0	0	0	0	0	0
0.2245	−89	−43	−20	−12	−6	−4	−2	−1
0.4084	−100	−49	−24	−14	−7	−5	−2	−1
0.5976	−80	−40	−20	−12	−6	−4	−2	−1
0.7675	−51	−25	−13	−7	−3	−2	−1	0
0.9292	−17	−8	−3	−2	0	0	1	1

checked by NMR spectroscopy, and its water content was found to be 96 ppm, measured by Karl Fischer titration.

The procedure for the synthesis of [emim][TFA] was analogous to that reported elsewhere.[25] Equimolar amounts of 1-ethyl-3-methylimidazolium bromide (Fluka, 97.0 %), further purified in our laboratory prior to use, and silver trifluoroacetate (Aldrich, 98 %), used as received, were dissolved in water. Both solutions were mixed and allowed to react for 24 h in a similar setup to that described for the synthesis of [emim][OTf]. The resulting solution was filtered to remove the AgBr precipitate, and water was partially eliminated in a rotary evaporator. The presence of bromide or silver anions in the product was tested, respectively, by addition of AgNO$_3$ and NaCl solutions to probe vials containing an aliquot of the reaction product. According to the precipitations observed in the tests, an additional amount of one of the starting materials was added in order to neutralize the excess of the other. The reaction and subsequent steps were repeated until no precipitate was observed in either of the tests. The purification was completed by drying the IL thoroughly under high vacuum at moderate temperature for several days. A water content of 128 ppm was assessed by Karl Fischer titration. High-purity water, deionized through a Milli-Q Water System, was used for all the experiments.

Mixtures of water and IL were prepared by mass using a Mettler Toledo AE 160 balance, precise to within $\pm 1 \times 10^{-4}$ g. Good mixing was ensured by magnetic stirring. All the samples were prepared immediately prior to performing density or viscosity measurements to avoid variations in composition due to evaporation of water or pickup of water by the hygroscopic IL.

Density Measurements. Densities were measured at atmospheric pressure in a DMA 4500 Anton Paar oscillating U-tube densitometer, which includes an automatic correction for the viscosity of the sample. The apparatus is precise to within 1×10^{-5} g·cm^{-3}, and the uncertainty of the measurements was estimated to be better than $\pm 5 \times 10^{-5}$ g·cm^{-3}. Two integrated Pt 100 platinum thermometers provided good precision (± 0.01 K) in temperature control internally.

Viscosity Measurements. Viscosity measurements were carried out in a Brookfield model DV-III Ultra Programmable (cone and plate) rheometer, with a nominal uncertainty of ± 2 %. Actual uncertainties for low viscosity samples with high water contents are greater than this, as described in the next paragraph. Temperature was controlled with a precision of ± 0.1 K by means of a TC-602 bath thermostat with a Brookfield temperature controller unit attached.

The measurement chamber for the viscometer is closed but not hermetically sealed from the atmosphere, so the time a sample spent in the chamber was kept to a minimum in order to reduce moisture uptake by the IL or loss of water by evaporation. However, the time required to ensure thermal equilibrium at each measured temperature was unavoidable, so variations in the concentration of the samples did occur, which introduces an additional experimental error in the viscosity data. Karl Fischer measurements on test samples before and after the viscosity measurements showed a rise in water content for pure IL samples and water loss for high water content mixtures. These variations were particularly significant at high temperatures, with water losses as great as 0.035 mass fraction observed. An additional complication is that the viscometer is significantly

Table 2. Experimental Density ρ, Excess Molar Volume V^E, Dynamic Viscosity η, and Viscosity Deviation $\Delta\eta$ for the Binary System Water (1) + [emim][OTf] (2)

x_1	T/K							
	278.15	288.15	298.15	308.15	318.15	328.15	338.15	348.15
ρ/g·cm^{-3}								
0.0000	1.40052	1.39204	1.38360	1.37522	1.36690	1.35863	1.35043	1.34230
0.2295	1.38830	1.37981	1.37136	1.36295	1.35459	1.34627	1.33801	1.32977
0.4310	1.37238	1.36387	1.35539	1.34693	1.33849	1.33007	1.32168	1.31329
0.6157	1.34734	1.33887	1.33037	1.32186	1.31333	1.30478	1.29619	1.28758
0.7825	1.29991	1.29174	1.28347	1.27510	1.26662	1.25804	1.24935	1.24055
0.8608	1.25476	1.24716	1.23938	1.23142	1.22327	1.21494	1.20643	1.19774
0.9353	1.17190	1.16597	1.15965	1.15294	1.14588	1.13849	1.13076	1.12273
0.9712	1.09749	1.09364	1.08908	1.08390	1.07818	1.07195	1.06525	1.05813
0.9924	1.03035	1.02864	1.02588	1.02224	1.01786	1.01283	1.00721	1.00105
1.0000	0.99999	0.99913	0.99707	0.99406	0.99023	0.98571	0.98056	0.97484
V^E/cm^3·mol^{-1}								
0.0000	0.000	0.000	0.000	0.000	0.000	0.000	0.000	0.000
0.2295	0.104	0.135	0.162	0.187	0.210	0.232	0.252	0.276
0.4310	0.062	0.120	0.170	0.216	0.260	0.302	0.343	0.385
0.6157	−0.040	0.037	0.106	0.170	0.230	0.287	0.346	0.404
0.7825	−0.123	−0.037	0.039	0.108	0.174	0.237	0.300	0.363
0.8608	−0.142	−0.061	0.008	0.071	0.131	0.188	0.243	0.299
0.9353	−0.124	−0.065	−0.016	0.027	0.067	0.105	0.142	0.179
0.9712	−0.075	−0.043	−0.016	0.007	0.028	0.049	0.069	0.088
0.9924	−0.018	−0.010	−0.003	0.002	0.008	0.013	0.018	0.024
1.0000	0.000	0.000	0.000	0.000	0.000	0.000	0.000	0.000
η/mPa·s								
0.0000	96	61	41	29	21	16	13	11
0.2286	47	32	23	17	13	10	9	7
0.4324	28	20	15	12	10	8	7	6
0.6159	18	13	10	8	7	6	5	5
0.7830	10	7	6	5	4	4	4	3
0.9352	5	4	3	3	3	3	2	2
$\Delta\eta$/mPa·s								
0.0000	0	0	0	0	0	0	0	0
0.2286	−27	−15	−9	−6	−4	−2	−1	−1
0.4324	−27	−15	−9	−5	−3	−1	−1	0
0.6159	−20	−11	−7	−4	−2	−1	0	1
0.7830	−12	−7	−4	−2	−1	0	1	1
0.9352	−3	−1	0	0	1	1	1	1

less accurate (i.e., greater than ± 2 % uncertainty) for viscosities below 5 mPa·s. Of course, the high water content samples have low viscosity, especially at high temperatures. Taking both these factors into consideration, we estimate the uncertainty in the measurements to be approximately ± 2 % for high viscosity samples but as much as ± 2 mPa·s for medium viscosity samples (between 50 and 100 mPa·s) and ± 1 mPa·s for low viscosity samples (below 50 mPa·s), which represents a considerably large relative error for the samples at high temperature and with high water content.

Results and Discussion

Experimental density ρ and dynamic viscosity η of the water + [emim][EtSO$_4$], water + [emim][OTf], and water + [emim][TFA] binary systems over the temperature range $T = (278.15$ to $348.15)$ K are reported in Tables 1 to 3. The densities and viscosities are highest for the pure ILs, with decreasing values with increasing water content. As expected, both density and viscosity decrease with increasing temperature. The density of pure water agrees with literature data within experimental error.[26] Comparison with the viscosity of pure water was not possible because the rheometer is not accurate at low viscosity.

Compared to literature, the density values for pure [emim][EtSO$_4$] are somewhat lower (by about 0.0045 g·cm^{-3}) than those reported by Krummen et al.[27] and Jacquemin et al.[28] and notably higher than those given by Yang et al.,[19,29] who do not report the water content of the IL. In the latter, measurements of the density of mixtures water + [emim][EtSO$_4$] are also carried out, which are again found to be systematically lower than the ones reported in the present work. These observations are consistent with the pure IL used by Yang et al. containing significant amounts of water, thus altering the true composition of the mixtures. We do not have any explanation for the small but significant discrepancy between our pure [emim][EtSO$_4$] data and that reported by Krummen et al.[27] and Jacquemin et al.[28] except possible different nonvolatile impurities in their samples or our samples from Solvent Innovation. We did repeat our measurements with a sample synthesized in our laboratory, with similar water content, and found values slightly higher (by approximately 0.0014 g·cm^{-3}) than those presented here for the Solvent Innovation sample, yet still a bit lower than the Krummen et al.[27] and Jacquemin et al.[28] data. We found no previous data as a function of temperature for [emim][OTf] or [emim][TFA] or their mixtures with water. No comparison is attempted with a few literature room temperature density values since the water contents were not reported.

Viscosity values at several temperatures were reported in the literature for pure [emim][EtSO$_4$] and [emim][OTf] by Jacquemin et al.[28] and Seddon et al.,[30] respectively, although using ILs with not exactly the same water content. Their values were found to be in reasonable agreement (within 6 % for the worst case throughout the entire temperature range studied here) with the values for the corresponding pure ILs in this paper.

Effect of Temperature on Density. Figure 1 shows the experimental densities for the three binary systems studied, as a function of temperature, for different compositions. As it can be observed, the density decreases as both temperature and water composition in the systems increase.

To the eye, the change in density with temperature for the pure ILs in Figure 1 looks linear. This linear behavior has

Table 3. Experimental Density ρ, Excess Molar Volume V^E, Dynamic Viscosity η, and Viscosity Deviation $\Delta\eta$ for the Binary System Water (1) + [emim][TFA] (2)

	T/K							
x_1	278.15	288.15	298.15	308.15	318.15	328.15	338.15	348.15
ρ/g·cm^{-3}								
0.0000	1.30689	1.29881	1.2908	1.28285	1.27495	1.26712	1.25935	1.25163
0.2050	1.29984	1.29182	1.28385	1.27592	1.26804	1.26021	1.25242	1.24466
0.3983	1.29127	1.28325	1.27526	1.26729	1.25934	1.25141	1.24349	1.23559
0.5808	1.278	1.26993	1.26185	1.25377	1.24567	1.23755	1.22941	1.22123
0.7573	1.24838	1.24021	1.23195	1.22366	1.2153	1.20684	1.19832	1.18998
0.8420	1.21687	1.20886	1.20076	1.19257	1.18427	1.17586	1.16733	1.15869
0.9256	1.15147	1.14467	1.13765	1.1304	1.12293	1.1152	1.10728	1.09905
0.9667	1.08688	1.08251	1.07755	1.07206	1.06608	1.05966	1.05283	1.04556
0.9912	1.02668	1.02493	1.02215	1.0185	1.01411	1.00907	1.00287	0.99723
1.0000	0.99999	0.99913	0.99707	0.99406	0.99023	0.98571	0.98056	0.97484
V^E/cm^3·mol^{-1}								
0.0000	0.000	0.000	0.000	0.000	0.000	0.000	0.000	0.000
0.2050	−0.112	−0.095	−0.080	−0.066	−0.055	−0.045	−0.034	−0.024
0.3983	−0.370	−0.331	−0.296	−0.265	−0.237	−0.209	−0.181	−0.154
0.5808	−0.651	−0.588	−0.532	−0.482	−0.435	−0.388	−0.343	−0.297
0.7573	−0.764	−0.675	−0.595	−0.524	−0.457	−0.392	−0.328	−0.278
0.8420	−0.698	−0.604	−0.523	−0.449	−0.382	−0.319	−0.257	−0.199
0.9256	−0.471	−0.392	−0.327	−0.270	−0.219	−0.171	−0.127	−0.083
0.9667	−0.236	−0.194	−0.160	−0.130	−0.104	−0.079	−0.056	−0.032
0.9912	−0.050	−0.042	−0.035	−0.030	−0.024	−0.019	−0.002	−0.007
1.0000	0.000	0.000	0.000	0.000	0.000	0.000	0.000	0.000
η/mPa·s								
0.0000	78	48	32	23	17	13	10	9
0.2042	56	35	24	17	13	10	8	7
0.3952	40	26	18	14	10	8	7	6
0.5808	25	17	12	9	8	6	6	5
0.7565	16	11	8	6	5	5	4	4
0.9256	6	5	4	3	3	3	2	2
$\Delta\eta$/mPa·s								
0.0000	0	0	0	0	0	0	0	0
0.2042	−7	−3	−2	−1	0	0	0	0
0.3952	−8	−4	−2	−1	0	0	1	1
0.5808	−8	−4	−2	−1	0	1	1	1
0.7565	−4	−2	−1	0	1	1	1	1
0.9256	−1	0	1	1	1	1	1	1

Table 4. Volume Expansivity α of Pure ILs for a 99 % Confidence Interval

	α/10^{-4} K^{-1}		
T/K	[emim][EtSO$_4$]	[emim][OTf]	[emim][TFA]
278.15	5.51 ± 0.03	6.087 ± 0.004	6.201 ± 0.002
288.15	5.50 ± 0.03	6.082 ± 0.005	6.193 ± 0.002
298.15	5.49 ± 0.03	6.076 ± 0.005	6.185 ± 0.002
308.15	5.48 ± 0.03	6.071 ± 0.005	6.177 ± 0.003
318.15	5.47 ± 0.03	6.065 ± 0.005	6.168 ± 0.003
328.15	5.46 ± 0.03	6.059 ± 0.005	6.159 ± 0.003
338.15	5.45 ± 0.03	6.052 ± 0.005	6.149 ± 0.003
348.15	5.43 ± 0.03	6.045 ± 0.006	6.139 ± 0.003

already been reported by several authors for pure ILs.[20,28] For the ILs in this work, the observation of such behavior will be discussed in more detail below in the section on volume expansivity of pure ILs.

By increasing the composition of water in the systems, the temperature dependence becomes distinctly nonlinear, especially at high water content. This is not surprising since the density of pure water is well-known to show nonlinear behavior with temperature. A second-order polynomial was found to satisfactorily correlate, from an empirical perspective, the change of density with temperature throughout the whole range of composition:

$$\rho = k_2 T^2 + k_1 T + k_0 \tag{1}$$

where T is for the absolute temperature and k_2, k_1, and k_0 refer to the fit coefficients. Least-square fits generated the values listed in Table S1 in the Supporting Information, where the magnitude of k_2 is an indication of the degree of curvature of density as a function of temperature for each given composition. From the standard deviation values given in Table S1, it is clear that the quality of the correlation decreases with increasing water concentration. However, even for pure water, the accuracy of the fit is acceptable for our purposes. Nevertheless, it must be noticed that the empirical correlation presented is not intended to provide an accurate description of the density of pure water itself, a task that is out of the scope of this work. The polynomial correlations are plotted with solid lines in Figure 1, along with the experimental data.

Volume Expansivity of the Pure ILs. For a pure fluid, the volume expansivity α, also known as the coefficient of thermal expansion, is a measure of how the volume changes with temperature. α is defined as[31]

$$\alpha = \frac{1}{V}\left(\frac{\partial V}{\partial T}\right)_p = -\frac{1}{\rho}\left(\frac{\partial \rho}{\partial T}\right)_p \tag{2}$$

where subscript p indicates constant pressure. It has already been shown in Figure 1 that the densities of pure ILs appear to decrease linearly ($R^2 > 0.9999$, standard deviation $\sigma < 0.00017$) with temperature (i.e., $(\partial\rho/\partial T)_p$ is a constant). From elemental calculus, it turns out that the right-hand term in eq 2 can be expressed as $-(\partial \ln \rho/\partial T)_p$. Not surprisingly, a plot of ln ρ as a function of temperature can also be fit by a straight line, with improved correlation coefficients ($R^2 > 0.99999$) and standard deviations ($\sigma < 0.00005$). According to this second perspective,

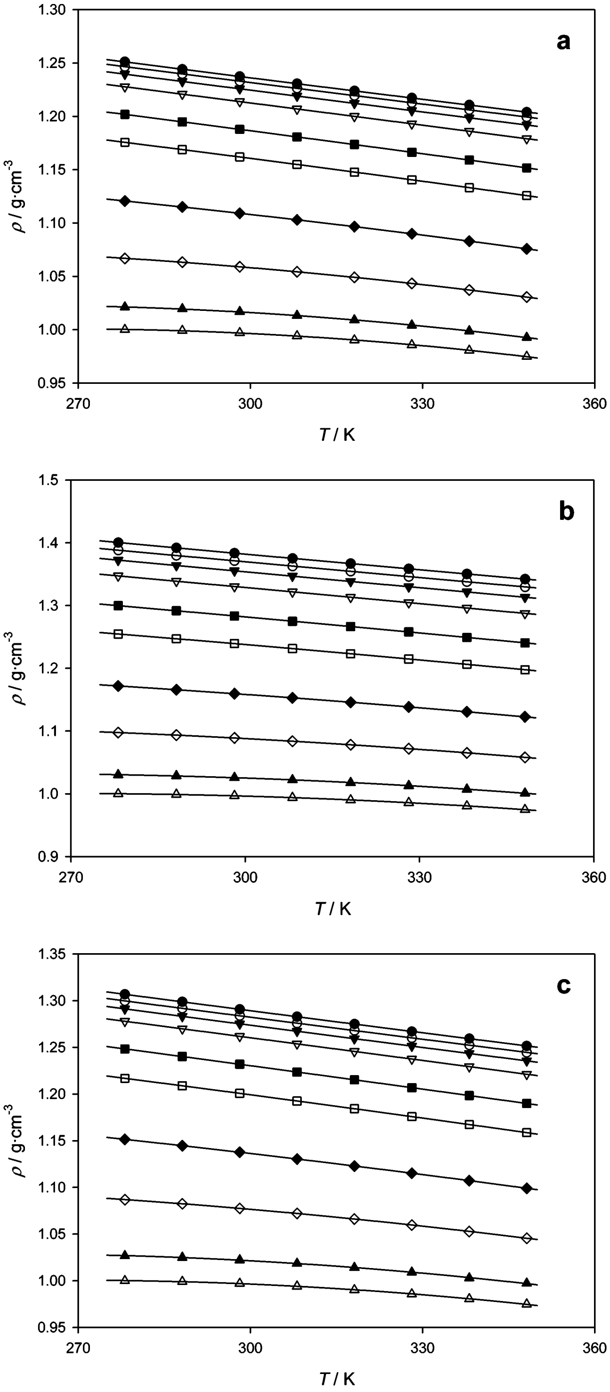

Figure 1. Density ρ for the water (1) + IL (2) binary systems as a function of temperature at different approximated mass fractions of water: ●, 0 %; ○, 2 %; ▼, 5 %; ▽, 10 %; ■, 20 %; □, 30 %; ◆, 50 %; ◇, 70 %; ▲, 90 %; △, 100 %. Polynomial correlations are plotted as solid lines. IL: (a) [emim][EtSO$_4$]; (b) [emim][OTf]; (c) [emim][TFA].

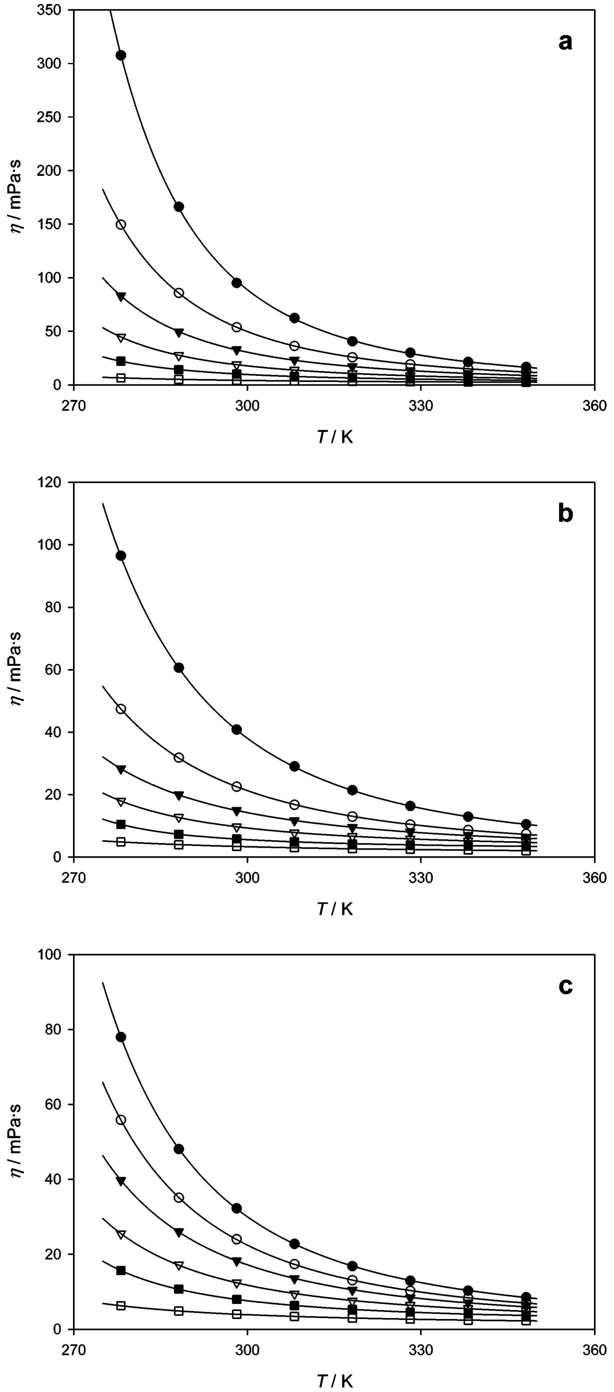

Figure 2. Dynamic viscosity η for the water (1) + IL (2) binary systems as a function of temperature at different approximated mass fractions of water: ●, 0 %; ○, 2 %; ▼, 5 %; ▽, 10 %; ■, 20 %; □, 50 %. The correlations performed with the VFT equation are plotted as solid lines. IL: (a) [emim][EtSO$_4$]; (b) [emim][OTf]; (c) [emim][TFA].

$(\partial \ln \rho/\partial T)_p$ is a constant. This seems to lead to conflicting results. If one considers a plot of ln ρ versus T to be linear, then α is a constant. If one considers a plot of ρ versus T to be linear, then the magnitude of α increases with increasing temperature because one must multiply the slope by the inverse of the density. In the literature, both alternatives can be found for the calculation of volume expansivities for ILs.[20,28,29,32]

A more careful examination reveals that the densities of the pure ILs measured here actually do not increase linearly with temperature. An analysis of the residuals indicates subtle but clear curvature for all three ILs. A second-order polynomial, of the type already used to fit the densities of the IL + water mixtures, provides a much better fit. A statistical analysis by means of the *F*-test showed that the addition of the quadratic term provided a statistically significant improvement in the fit at a significance level of 0.05 for the water + [emim][EtSO$_4$] system and at significance levels as low as 0.001 for the other two binary systems. The fit parameters are shown in Table S1 in the Supporting Information. The partial derivative in the right-hand side of eq 2 can be evaluated from the polynomial fits, and the corresponding volume expansivity values can be calculated. The results are summarized in Table 4.

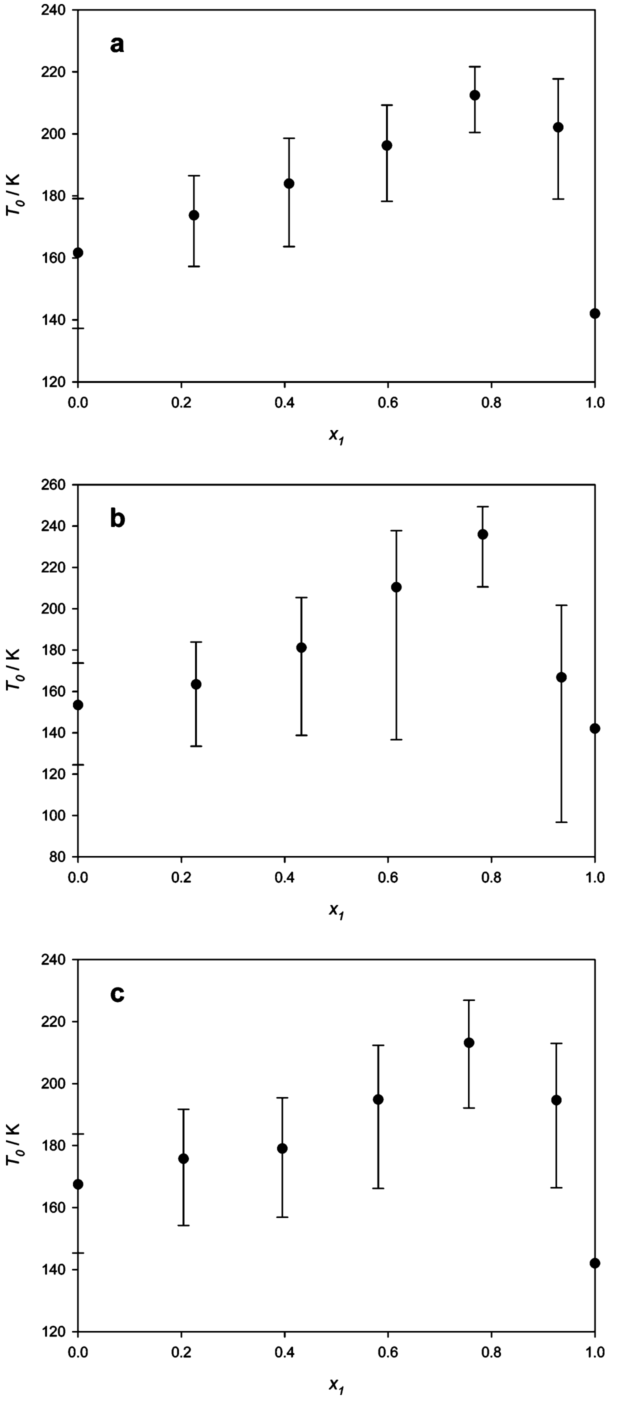

Figure 3. Ideal glass transition temperature T_0 for the water (1) + IL (2) systems, as obtained from the VFT equation correlations. IL: (a) [emim][EtSO$_4$]; (b) [emim][OTf]; (c) [emim][TFA].

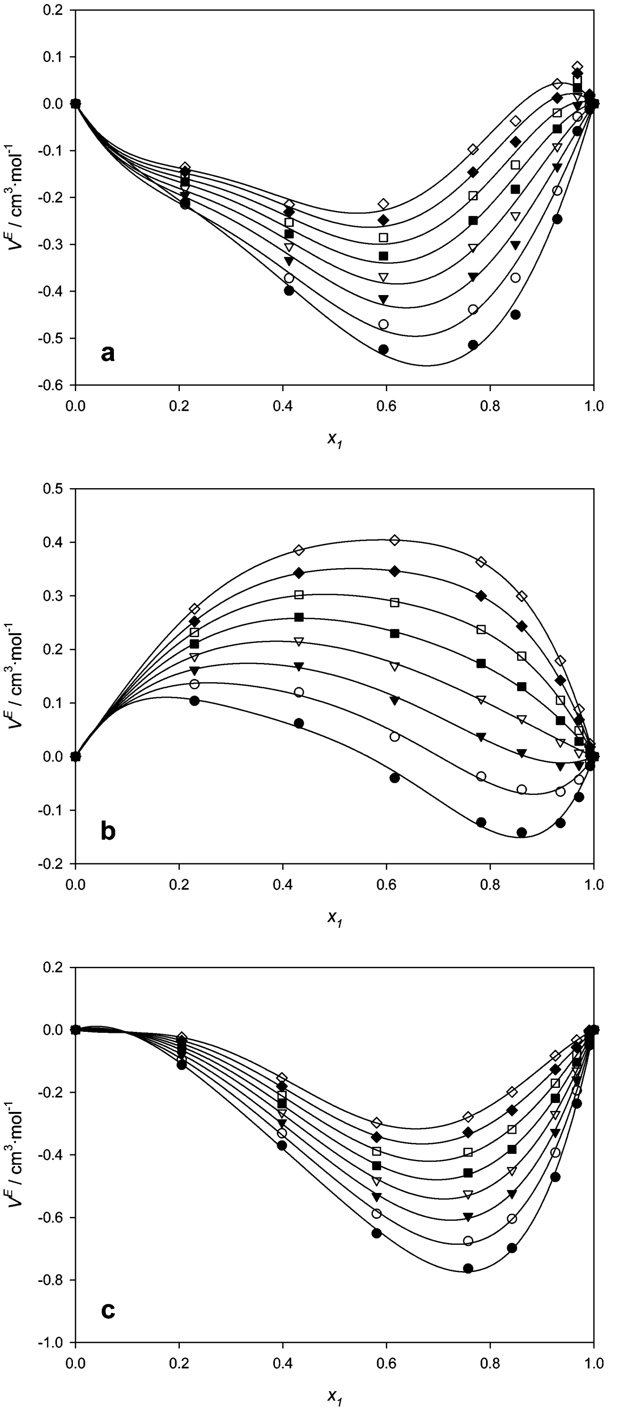

Figure 4. Excess molar volume V^E for the water (1) + IL (2) systems at different temperatures: ●, 278.15 K; ○, 288.15 K; ▼, 298.15 K; ▽, 308.15 K; ■, 318.15 K; □, 328.15 K; ◆, 338.15 K; ◇, 348.15 K. The solid lines represent the corresponding correlations by the Redlich−Kister equation. IL: (a) [emim][EtSO$_4$]; (b) [emim][OTf]; (c) [emim][TFA].

The volume expansivities calculated from the polynomial fits and eq 2 are almost constant, just decreasing slightly with increasing temperature for all three ILs. Actually, the constant values obtained by assuming that a plot of ln ρ versus temperature is linear provide good estimates: 5.48×10^{-4} K^{-1} for [emim][EtSO$_4$], 6.07×10^{-4} K^{-1} for [emim][OTf], and 6.17×10^{-4} K^{-1} for [emim][TFA]. Nonetheless, the values shown in Table 4, which do decrease with increasing temperature, are the best analysis of the experimental data. These comparisons emphasize that it is important to carefully analyze the experimental data in order to avoid corruption of the thermodynamic concepts or misrepresentation of the experimental data. In addition, if analyzed with one of the linear approximations, one should not make major distinctions in whether α is increasing, constant, or decreasing with temperature for these systems since this is highly dependent on how the data are analyzed.

In general, values in Table 4 are within the common range reported for ILs in the literature (roughly around 5×10^{-4} to 8×10^{-4} K^{-1}), being somewhat lower than typical expansivities for conventional molecular solvents.[32,33] A specific comparison of the results is possible for [emim][EtSO$_4$] as three other research groups have studied the density variation of this pure IL with temperature. Our values for [emim][EtSO$_4$] are certainly close to the constant of 5.37×10^{-4} K^{-1} reported by Yang et

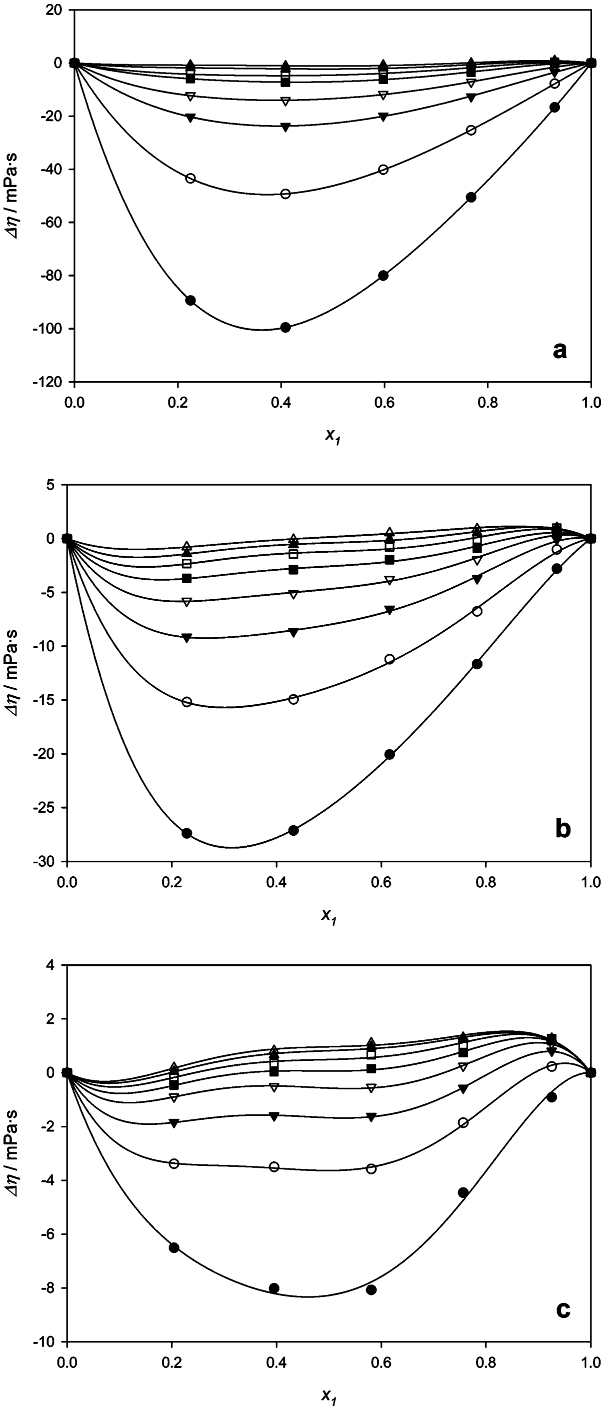

Figure 5. Viscosity deviation $\Delta\eta$ for the water (1) + IL (2) systems at different temperatures: ●, 278.15 K; ○, 288.15 K; ▼, 298.15 K; ▽, 308.15 K; ■, 318.15 K; □, 328.15 K; ▲, 338.15 K; △, 348.15 K. The solid lines represent the corresponding correlations by the Redlich−Kister equation. IL: (a) [emim][EtSO$_4$]; (b) [emim][OTf]; (c) [emim][TFA].

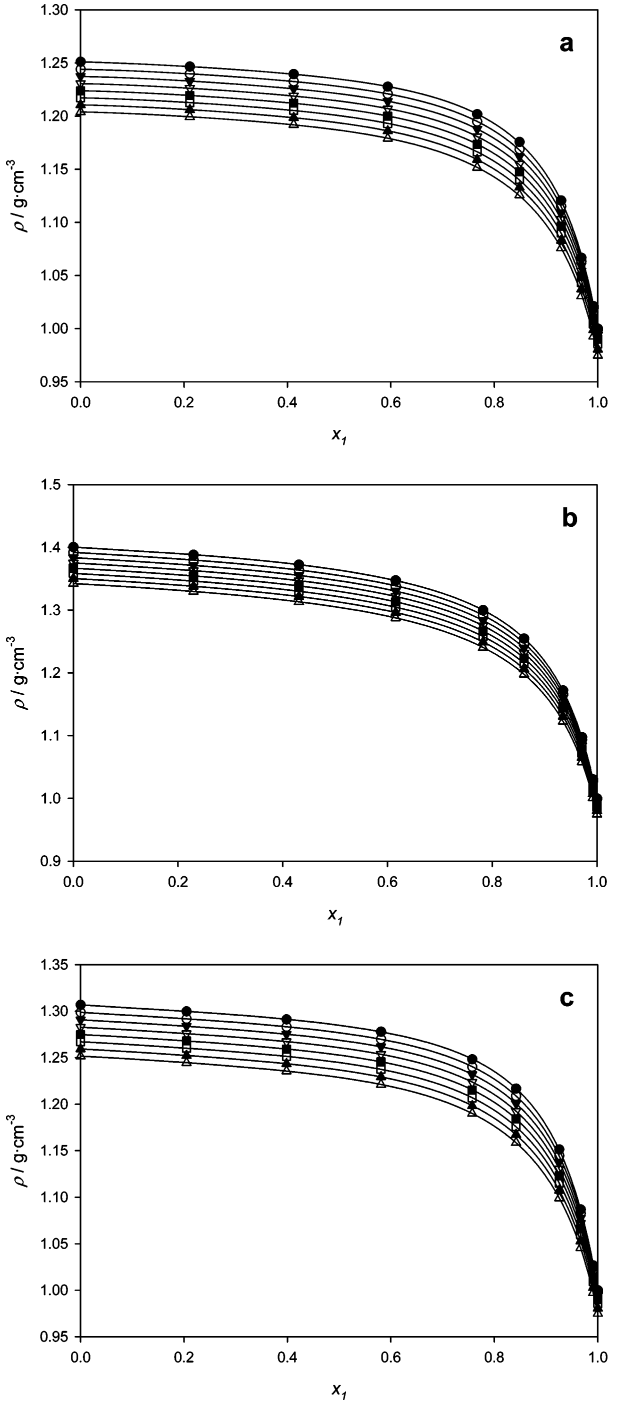

Figure 6. Density ρ for the water (1) + IL (2) systems, as a function of mole fraction of water, at different temperatures: ●, 278.15 K; ○, 288.15 K; ▼, 298.15 K; ▽, 308.15 K; ■, 318.15 K; □, 328.15 K; ▲, 338.15 K; △, 348.15 K. The solid lines correspond to the fits derived from the Redlich−Kister correlation of the excess molar volume V^E. IL: (a) [emim][EtSO$_4$]; (b) [emim][OTf]; (c) [emim][TFA].

al.[29] However, they are significantly higher than those reported by Jacquemin et al.[28]: 4.82 × 10^{-4} K^{-1} at 293.15 K and 4.94 × 10^{-4} K^{-1} at 343.15 K. These authors report increasing volume expansivity with increasing temperature, the opposite of the trend we report, but as explained above, this is simply because they fit ρ versus T with a straight line. As mentioned above, our data show a clear convex curvature, which is well fit by a second-order polynomial. A similar curvature is present in the density data reported by Yang et al. and Krummen et al.[27] for [emim][EtSO$_4$]. By fitting Krummen's raw data to a second-order polynomial and calculating the volume expansivity according to eq 2, one obtains values of (5.62 to 5.47) × 10^{-4} K^{-1} at temperatures from (293.15 to 353.15) K, in good agreement with our values.

Interestingly, the detailed analysis of the data performed here indicates that the three ILs studied in this work actually show decreasing volume expansivity with increasing temperature. This is a very unusual behavior for fluids in general. Of course, it is contrary to the results reported for other ILs,[33,34] but this is not surprising since assumptions of linearity in fitting the data can affect the results, as explained above. Rebelo et al.[17] speculated

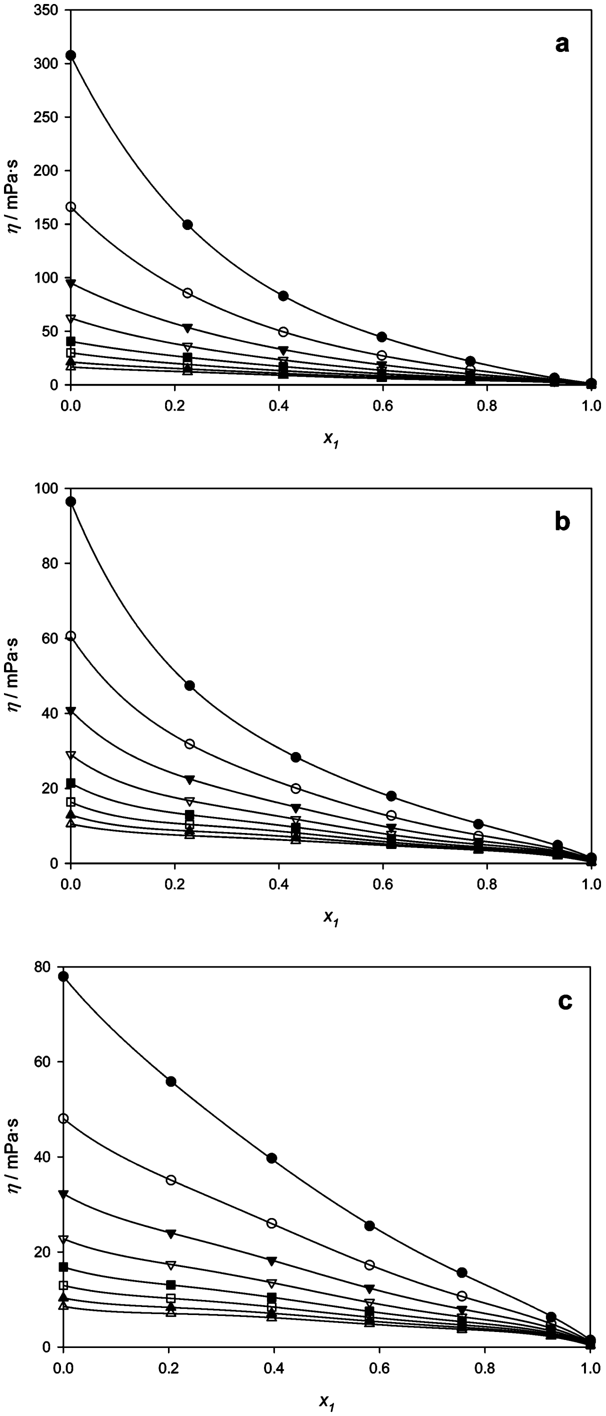

Figure 7. Viscosity η for the water (1) + IL (2) systems, as a function of mole fraction of water, at different temperatures: ●, 278.15 K; ○, 288.15 K; ▼, 298.15 K; ▽, 308.15 K; ■, 318.15 K; □, 328.15 K; ▲, 338.15 K; △, 348.15 K. The solid lines correspond to the fits derived from the Redlich−Kister correlation of the viscosity deviation $\Delta\eta$. IL: (a) [emim][EtSO$_4$]; (b) [emim][OTf]; (c) [emim][TFA].

about the possibility of finding ILs following such behavior, which, in accord with thermodynamic relationships, implies the unusual situation that their molar heat capacities will increase with increasing pressure. Since volume expansivity must rise to $+\infty$ as the critical point of a substance is approached, a minimum in α must appear at higher temperatures than those investigated here, unless obscured by decomposition of the ILs. While decreasing volume expansivity with increasing temperature may not be general for all ILs, it is interesting that all three ILs investigated here, which contain the rather different [EtSO$_4$]$^-$, [OTf]$^-$, and [TFA]$^-$ anions, exhibit this behavior.

Effect of Temperature on Viscosity. The values of viscosity as a function of temperature for binary mixtures of different compositions for the three water + IL systems are depicted in Figure 2. The well-known Arrhenius-type equation has been widely used to correlate variations of viscosity with temperature in liquids:

$$\eta = \eta_\infty \exp\left(-\frac{E_a}{RT}\right) \tag{3}$$

where R is the universal gas constant and the characteristic parameters are η_∞ (viscosity at infinite temperature) and E_a ("activation" energy). However, for ILs it has been reported[35] that a better description is provided by the modified version[36] of the Vogel−Fulcher−Tammann (VFT) equation,[37−39] which characterizes glass-forming liquids:

$$\eta = AT^{0.5} \exp\left(\frac{k}{T - T_0}\right) \tag{4}$$

The fit parameters are A, k, and T_0. It was originally proposed as an entirely empirical equation, but the development of the free volume theory of Cohen and Turnbull[36] and the configurational entropy approach of Adam and Gibbs[40] convey some theoretical significance to the parameter T_0. It is the "ideal glass transition temperature", a temperature below which the fluid exists as an equilibrium glass where the mass-transporting motions are frozen out.[41] For kinetic reasons, T_0 cannot be reached in a finite time scale experiment; however, it should be slightly below the experimental glass transition temperature T_g.[42]

The VFT equation suitably correlates, as a function of the temperature, not only the viscosities of the pure ILs but also the viscosities of the mixtures for the binary systems throughout the composition range. The significant improvement in the data fit by the VFT equation over the Arrhenius equation can be noticed by comparison of the relative standard deviations listed in Table S2 in the Supporting Information, along with the adjusted parameters for the correlations with each equation. This, of course, is not unexpected since the VFT contains three parameters compared to two for the Arrhenius equation. The VFT fits are plotted with the experimental data in Figure 2.

Figure 3 shows T_0 as a function of composition for the three water + IL systems. Since the adjustable parameters are very sensitive to small changes in the viscosity data, large variations in the fit values of T_0 occur simply as a result of the experimental error. Therefore, error bars were estimated and are included in the plot. For pure water, the value of T_0 was obtained from viscosity data taken from literature,[26] correlated by means of the VFT equation. T_0 increases with increasing water concentration for all three water + IL systems, reaching a maximum at about 0.8 mole fraction of water. While the large asymmetry in molecular size and the complexity of the IL may complicate the analysis, for systems of small molecules and ionic species the most important factor in setting the magnitude of T_0 (or T_g) is the overall cohesive energy of the liquid mixture.[41] Thus, the plots in Figure 3 imply that the interactions between water and the ILs are maximized in mixtures with an IL mole fraction of approximately 0.20. While this may be inferring too much meaning from a largely empirical equation, the similarity in the behavior of T_0 for the three systems is noteworthy.

The viscosity data for all three pure ILs resulted in similar values of T_0, in the range of (150 to 170) K. Comparison with

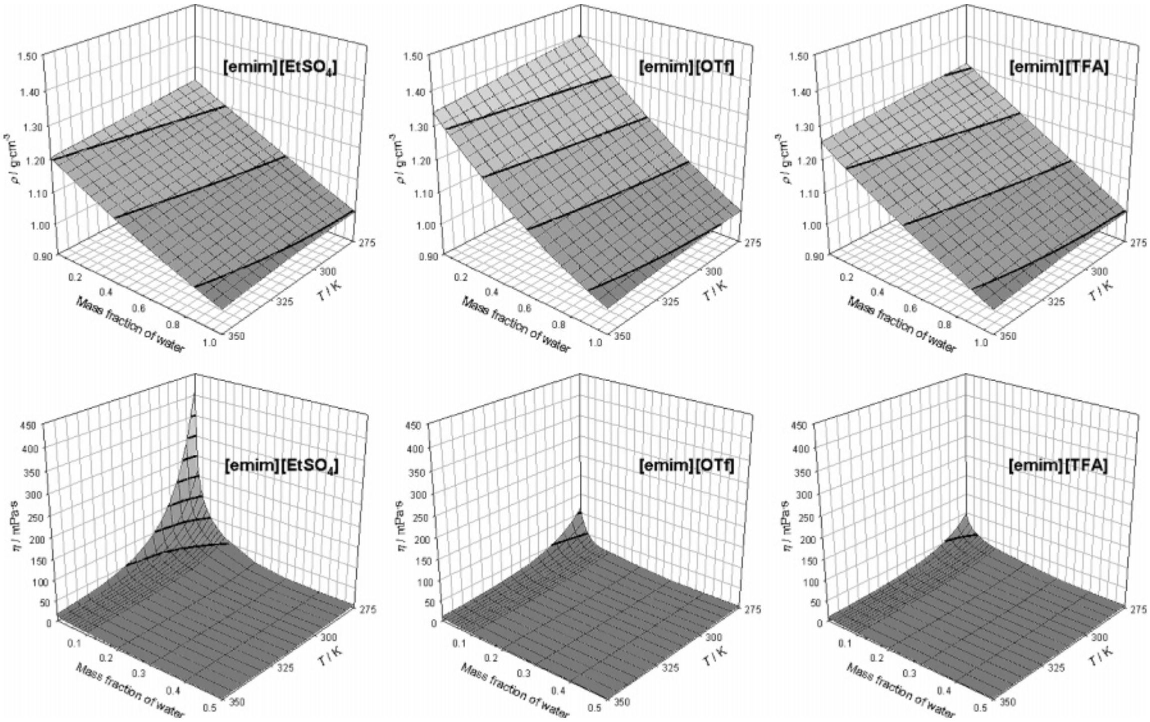

Figure 8. Pseudo-quantitative change of (a) density ρ and (b) viscosity η with temperature and composition for the water + IL binary systems. The left plots correspond to the IL [emim][EtSO$_4$]; the central plots correspond to [emim][OTf]; and the right plots correspond to [emim][TFA].

experimental T_g values is possible for [emim][EtSO$_4$], with literature T_g data ranging from (181 to 208) K.[43,44] Experimental discrepancies are no doubt due to varying concentrations of impurities, including water. Nonetheless, the experimental T_g values are somewhat greater than T_0 calculated from the viscosity data, consistent with the theoretical rationale for the VFT equation.

The parameters A and k in eq 4 change smoothly with composition for all three water + IL systems, as shown in Table S2 in the Supporting Information. However, their analysis will not be detailed here, as the physical meaning of these parameters is not so clear and their values are strongly sensitive to the choice of T_0.

Effect of Composition on Density and Viscosity. The excess molar volume, V^E, and viscosity deviation, $\Delta\eta$, were calculated from the experimental data for all the water + IL mixtures according to the following equations:

$$V^E = \sum x_i M_i \left(\frac{1}{\rho} - \frac{1}{\rho_i}\right) \tag{5}$$

$$\Delta\eta = \eta - \sum x_i \eta_i \tag{6}$$

where ρ and η are the density and viscosity of the solution and ρ_i and η_i refer to the density and viscosity of the pure component i. For the application of eq 6, water viscosity data were taken from reference literature[26] because our viscometer has large uncertainties for low viscosity samples, as explained in the Experimental Section. The results are listed in Tables 1 to 3. The excess volumes and viscosity deviations were fit for each temperature with a Redlich−Kister polynomial:[45]

$$Q = x_w x_{IL} \sum_{i=0}^{m} A_i (x_w - x_{IL})^i \tag{7}$$

where Q represents either the excess molar volume V^E or the viscosity deviation $\Delta\eta$, A_i is the fit parameters, and m is the degree of the polynomial expansion. A third-order polynomial was found to be the optimum for both properties. The fit parameters are summarized in Tables S3 and S4 in the Supporting Information along with the corresponding standard deviations for the correlations. The values of V^E and $\Delta\eta$ as well as the Redlich−Kister fits are plotted in Figures 4 and 5.

The graphs of V^E shown in Figure 4 indicate that mixtures of water with [emim][EtSO$_4$] and [emim][TFA] exhibit mostly negative deviations from ideality. The magnitude of the excess volume decreases with increasing temperature. Notable are the small positive deviations from ideality for dilute aqueous solutions of [emim][EtSO$_4$], which are not described very well by the Redlich−Kister correlation. In stark contrast is the behavior of the system water + [emim][OTf]. It exhibits mostly positive values of the excess volume, except at the lowest temperatures, where V^E is slightly positive for IL-rich compositions and slightly negative for water-rich compositions. The [OTf]$^-$ anion is known to be less hydrophilic than [EtSO$_4$]$^-$ or [TFA]$^-$.[8] Therefore, the probable explanation is that [emim][EtSO$_4$] and [emim][TFA] have stronger interactions with water, resulting in negative excess volumes, while the weaker interactions with [emim][OTf] are insufficient to cause volume contraction. The decrease in the magnitude of the negative V^E values and the increase in the magnitude of the positive V^E values with increasing temperature can be attributed to the decreasing importance of hydrogen bonding with increasing temperature. Note that the slight positive values in the modeling for water + [emim][TFA] are not corroborated by any experimental data and should be taken lightly.

All of the excess molar volumes reported here are relatively small in comparison to the molar volume. As a consequence, it may be possible to correlate the molar volumes of water + IL systems with a straight line.[17] Although this may not be satisfying conceptually, it may be a valuable tool in practice for the quick calculation of densities of binary water + IL systems.

The water + $[\text{emim}][\text{EtSO}_4]$ and water + [emim][OTf] systems show strong negative viscosity deviations at low temperatures, as shown in Figure 5. Although they show similar trends, the viscosity deviations for the water + [emim][TFA] system are not significantly greater than the uncertainty in the measurements. As the temperature increases, the deviations are reduced and even reach slightly positive values. The largest magnitude deviations occur for the system with the highest viscosity—$[\text{emim}][\text{EtSO}_4]$. In general, the Redlich−Kister fit provides a good description of the change in $\Delta\eta$ with composition for all three systems.

Using the correlation of the excess properties by the Redlich−Kister polynomials, the absolute values of the densities and viscosities of the binary system can be expressed as simple functions of composition. By combining eq 7 with eqs 5 and 6, analytical expressions are obtained for ρ and η. Both the experimental data and the correlations are shown in Figures 6 and 7. Note how a few moles of IL added to pure water dramatically increases the density of the mixtures, while the most pronounced effect on viscosity occurs when adding water to pure IL, especially at low temperatures.

Combined Effect of Temperature and Composition. Above we have presented experimental data and correlations of the density and viscosity of the three water + IL systems as a function of temperature and as a function of composition. If, for instance, one analyzes the parameters in the temperature-dependent fit as a function of composition, then it is possible to combine the correlations and build a three-dimensional plot of the physical property as a function of both temperature and composition. Such plots are shown in Figure 8. They provide a quick visualization of the combined influence of temperature and composition on the density and viscosity for the three water + IL binary systems studied in this work. The scales are the same for all three systems in order to allow an easy comparison between the ILs. Although a mole basis is usually preferred for thermodynamic analysis of mixtures, the significant difference between the molecular weight of water and the formula weights of the ILs makes presentation on a mass fraction basis of interest, and this is what is shown in Figure 8. Note that the viscosity plots only extend to a water mass fraction of 50 %, which is the highest water composition investigated.

It is clear that composition has a greater influence than temperature on density. For viscosity, dramatic decreases are observed with the addition of small masses of water, especially at low temperature. Hence, these graphs emphasize the extreme sensitivity of pure IL viscosity to water content.[8] From a practical standpoint, this means that highly viscous solutions of IL and water can be circumvented simply by avoiding temperatures close to the freezing point of water or streams with very low water content.

Conclusions

The density and viscosity of binary mixtures of water + $[\text{emim}][\text{EtSO}_4]$, water + [emim][OTf], and water + [emim][TFA] were investigated at atmospheric pressure from (278.15 to 348.15) K. Both properties were found to decrease with an increase in either temperature or in mole fraction of water. An empirical second-order polynomial and the VFT equation were used to correlate, respectively, density and viscosity as a function of the absolute temperature. Reasonable correlations of the composition dependence were achieved by fitting the excess molar volumes and the viscosity deviations to third-order Redlich−Kister polynomials. Viscosity is more sensitive than density to changes in temperature or composition; this behavior is especially critical at low temperatures or low water concentrations, where dramatic variations of viscosity occur.

The ILs incorporating the fluorinated $[\text{OTf}]^-$ and $[\text{TFA}]^-$ anion lead to higher densities and lower viscosities than the one with the non-fluorinated $[\text{EtSO}_4]^-$ anion. Nevertheless, economical and even environmental considerations should also be taken into account before establishing the best IL for a given application involving these kinds of binary mixtures.

Supporting Information Available:

Fit parameters and standard deviation for the empirical correlation of density in the systems water + IL as a function of temperature (Table S1); fit parameters of the Arrhenius equation and the VFT equation, as well as their relative standard deviations, for the correlation of viscosity as a function of temperature in the systems water + IL (Table S2); coefficients of the Redlich−Kister equation for the correlation of the excess molar volume of the systems water + IL, along with the standard deviations (Table S3); and coefficients of the Redlich−Kister equation for the correlation of the viscosity deviation of the systems water + IL, along with the standard deviations (Table S4). This material is available free of charge via the Internet at http://pubs.acs.org.

Literature Cited

(1) Rogers, R. D.; Seddon, K. R. Ionic liquids—solvents of the future? *Science* **2003**, *302*, 792−793.

(2) Seddon, K. R. Ionic liquids: a taste of the future. *Nat. Mater.* **2003**, *2*, 363−365.

(3) Brennecke, J. F.; Maginn, E. J. Ionic liquids: innovative fluids for chemical processing. *AIChE J.* **2001**, *47*, 2384−2389.

(4) Blanchard, L. A.; Hancu, D.; Beckman, E. J.; Brennecke, J. F. Green processing using ionic liquids and CO_2. *Nature* **1999**, *399*, 28−29.

(5) Blanchard, L. A.; Brennecke, J. F. Recovery of organic products from ionic liquids using supercritical carbon dioxide. *Ind. Eng. Chem. Res.* **2001**, *40*, 287−292.

(6) Blanchard, L. A.; Gu, Z.; Brennecke, J. F. High-pressure phase behavior of ionic liquid/CO_2 systems. *J. Phys. Chem. B* **2001**, *105*, 2437−2444.

(7) Scurto, A. M.; Aki, S. N. V. K.; Brennecke, J. F. CO_2 as a separation switch for ionic liquid/organic mixtures. *J. Am. Chem. Soc.* **2002**, *124*, 10276−10277.

(8) Seddon, K. R.; Stark, A.; Torres, M. J. Influence of chloride, water, and organic solvents on the physical properties of ionic liquids. *Pure Appl. Chem.* **2000**, *72*, 2275−2287.

(9) Gaillon, L.; Sirieix-Plenet, J.; Letellier, P. Volumetric study of binary solvent mixtures constituted by amphiphilic ionic liquids at room temperature (1-alkyl-3-methylimidazolium bromide) and water. *J. Solution Chem.* **2004**, *33*, 1333−1347.

(10) Lu, X.-M.; Xu, W.-G.; Gui, J.-S.; Li, H.-W.; Yang, J. -Z. Volumetric properties of room temperature ionic liquid. 1. The system {1-methyl-3-ethylimidazolium ethyl sulfate + water} at temperature in the range (278.15 to 333.15) K. *J. Chem. Thermodyn.* **2005**, *37*, 13−19.

(11) Zafarani-Moattar, M. T.; Shekaari, H. Apparent molar volume and isentropic compressibility of ionic liquid 1-butyl-3-methylimidazolium bromide in water, methanol, and ethanol at T = (298.15 to 318.15) K. *J. Chem. Thermodyn.* **2005**, *37*, 1029−1035.

(12) Fitchett, B. D.; Knepp, T. N.; Conboy, J. C. 1-Alkyl-3-methylimidazolium bis(perfluoroalkylsulfonyl)imide water-immiscible ionic liquids. The effect of water on electrochemical and physical properties. *J. Electrochem. Soc.* **2004**, *151*, E219−E225.

(13) Pandey, S.; Fletcher, K. A.; Baker, S. N.; Baker, G. A. Correlation between the fluorescent response of microfluidity probes and the water content and viscosity of ionic liquid and water mixtures. *Analyst* **2004**, *129*, 569−573.

(14) Widegren, J. A.; Laesecke, A.; Magee, J. W. The effect of dissolved water on the viscosities of hydrophobic room-temperature ionic liquids. *Chem. Commun.* **2005**, 1610−1612.

(15) Chakrabarty, D.; Chakraborty, A.; Seth, D.; Sarkar, N. Effect of water, methanol, and acetonitrile on solvent relaxation and rotational relaxation of coumarin 153 in neat 1-hexyl-3-methylimidazolium hexafluorophosphate. *J. Phys. Chem. A* **2005**, *109*, 1764−1769.

(16) Zhang, S.; Li, X.; Chen, H.; Wang, J.; Zhang, J.; Zhang, M. Determination of physical properties for the binary system of 1-ethyl-3-methylimidazolium tetrafluoroborate + H_2O. *J. Chem. Eng. Data* **2004**, *49*, 760−764.

(17) Rebelo, L. P. N.; Najdanovic-Visak, V.; Visak, Z. P.; Nunes. da Ponte, M.; Szydlowski, J.; Cerdeiriña, C. A.; Troncoso, J.; Romaní, L.;

Esperança, J. M. S. S.; Guedes, H. J. R.; de Sousa, H. C. A detailed thermodynamic analysis of [C_4mim][BF_4] + water as a case study to model ionic liquid aqueous solutions. *Green Chem.* **2004**, *6*, 369−381.

(18) Xu, H.; Zhao, D.; Xu, P.; Liu, F.; Gao, G. Conductivity and viscosity of 1-allyl-3-methyl-imidazolium chloride + water and + ethanol from 293.15 K to 333.15 K. *J. Chem. Eng. Data* **2005**, *50*, 133−135.

(19) Yang, J.-Z.; Lu, X.-M.; Gui, J.-S.; Xu, W.-G.; Li, H. -W. Volumetric properties of room temperature ionic liquid. 2. The concentrated aqueous solutions of {1-methyl-3-ethylimidazolium ethyl sulfate + water} in a temperature range of 278.2 to 333.2 K. *J. Chem. Thermodyn.* **2005**, *37*, 1250−1255.

(20) Gómez, E.; González, B.; Domínguez, Á.; Tojo, E.; Tojo, J. Dynamic viscosities of a series of 1-alkyl-3-methylimidazolium chloride ionic liquids and their binary mixtures with water at several temperatures. *J. Chem. Eng. Data* **2006**, *51*, 696−701.

(21) Jarosik, A.; Krajewski, S. R.; Lewandowski, A.; Radzimski, P. Conductivity of ionic liquids in mixtures. *J. Mol. Liq.* **2006**, *123*, 43−50.

(22) Zhou, Q.; Wang, L.-S.; Chen, H.-P. Densities and viscosities of 1-butyl-3-methylimidazolium tetrafluoroborate + H_2O binary mixtures from (303.15 to 353.15) K. *J. Chem. Eng. Data* **2006**, *51*, 905−908.

(23) Archer, D. G.; Widegren, J. A.; Kirklin, D. R.; Magee, J. W. Enthalpy of solution of 1-octyl-3-methylimidazolium tetrafluoroborate in water and in aqueous sodium fluoride. *J. Chem. Eng. Data* **2005**, *50*, 1484−1491.

(24) Holbrey, J. D.; Reichert, W. M.; Swatloski, R. P.; Broker, G. A.; Pitner, W. R.; Seddon, K. R.; Rogers, R. D. Efficient, halide free synthesis of new, low cost ionic liquids: 1,3-dialkylimidazolium salts containing methyl- and ethyl-sulfate anions. *Green Chem.* **2002**, *4*, 407−413.

(25) Bonhôte, P.; Dias, A.-P.; Armand, M.; Papageorgiou, N.; Kalyanasundaram, K.; Grätzel, M. Hydrophobic, highly conductive ambient-temperature molten salts. *Inorg. Chem.* **1996**, *35*, 1168−1178. (Correction: *Inorg. Chem.* **1998**, *37*, 166).

(26) Riddick, J. A.; Bunger, W. B.; Sakano, T. K. *Organic Solvents: Physical Properties and Methods of Purification*, 4th ed.; John Wiley & Sons: New York, 1986.

(27) Krummen, M.; Wasserscheid, P.; Gmehling, J. Measurement of activity coefficients at infinite dilution in ionic liquids using the dilutor technique. *J. Chem. Eng. Data* **2002**, *47*, 1411−1417.

(28) Jacquemin, J.; Husson, P.; Padua, A. A. H.; Majer, V. Density and viscosity of several pure and water-saturated ionic liquids. *Green Chem.* **2006**, *8*, 172−180.

(29) Yang, J.-Z.; Lu, X.-M.; Gui, J.-S.; Xu, W. -G. A new theory for ionic liquids—the interstice model. Part 1. The density and surface tension of ionic liquid EMISE. *Green Chem.* **2004**, *6*, 541−543.

(30) Seddon, K. R.; Stark, A.; Torres, M.-J. Viscosity and density of 1-alkyl-3-methylimidazolium ionic liquids. *ACS Symp. Ser.* **2002**, *No. 819* (Clean Solvents: Alternative Media for Chemical Reactions and Processing), 34−49.

(31) Smith, J. M.; Van Ness, H. C.; Abbott, M. M. *Introduction to Chemical Engineering Thermodynamics*, 6th ed.; McGraw-Hill: New York, 2001.

(32) Gu, Z.; Brennecke, J. F. Volume expansivities and isothermal compressibilities of imidazolium- and pyridinium-based ionic liquids. *J. Chem. Eng. Data* **2002**, *47*, 339−345.

(33) Rebelo, L. P. N.; Najdanovic-Visak, V.; Gomes de Azevedo, R.; Esperança, J. M. S. S.; Nunes da Ponte, M.; Guedes, H. J. R.; Visak, Z. P.; de Sousa, H. C.; Szydlowski, J.; Canongia Lopes, J. N.; Cordeiro, T. C. Phase behavior and thermodynamic properties of ionic liquids, ionic liquid mixtures, and ionic liquid solutions. *ACS Symp. Ser.* **2005**, *No. 901* (Ionic Liquids IIIA: Fundamentals, Progress, Challenges, and Opportunities), 270−291.

(34) Marsh, K. N.; Boxall, J. A.; Lichtenthaler, R. Room temperature ionic liquids and their mixtures—a review. *Fluid Phase Equilib.* **2004**, *219*, 93−98.

(35) Wilkes, J. S. Properties of ionic liquid solvents for catalysis. *J. Mol. Catal. A* **2004**, *214*, 11−17.

(36) Cohen, M. H.; Turnbull, D. Molecular transport in liquids and glasses. *J. Chem. Phys.* **1959**, *31*, 1164−1169.

(37) Vogel, H. Das Temperatur-abhängigkeitsgesetz der Viskosität von Flüssigkeiten. *Phys. Z.* **1921**, *22*, 645−646.

(38) Fulcher, G. S. Analysis of recent measurements of the viscosity of glasses. *Am. Ceram. Soc. J.* **1925**, *8*, 339−355.

(39) Tammann, G.; Hesse, W. Die Abhängigkeit der Viscosität von der Temperatur bei unterkühlten Flüssigkeiten. *Z. Anorg. Allg. Chem.* **1926**, *156*, 245−257.

(40) Adam, G.; Gibbs, J. H. On the temperature dependence of cooperative relaxation properties in glass-forming liquids. *J. Chem. Phys.* **1965**, *43*, 139−146.

(41) Angell, C. A.; Moynihan, C. T. Transport processes in low-melting molten salt systems. In *Molten Salts: Characterization and Analysis*; Mamantov, G., Ed.; Marcel Dekker: New York, 1969.

(42) Gibbs, J. H.; DiMarzio, E. A. Nature of the glass transition and the glassy state. *J. Chem. Phys.* **1958**, *28*, 373−383.

(43) Holbrey, J. D.; Reichert, W. M.; Swatloski, R. P.; Broker, G. A.; Pitner, W. R.; Seddon, K. R.; Rogers, R. D. Efficient, halide free synthesis of new, low cost ionic liquids: 1,3-dialkylimidazolium salts containing methyl- and ethyl-sulfate anions. *Green Chem.* **2002**, *4*, 407−413.

(44) Strehmel, V.; Laschewsky, A.; Wetzel, H.; Görnitz, E. Free radical polymerization of *n*-butyl methacrylate in ionic liquids. *Macromolecules* **2006**, *39*, 923−930.

(45) Redlich, O.; Kister, A. T. Thermodynamics of nonelectrolyte solutions. Algebraic representation of thermodynamic properties and the classification of solutions. *Ind. Eng. Chem.* **1948**, *40*, 345−348.

Received for review June 20, 2006. Accepted August 25, 2006. We acknowledge funding for this project from the U.S. Department of Energy, under Grant FG02-05CH11294. H.R. is grateful to the Ministerio de Educación y Ciencia (Spain) for the FPI grant with reference BES-2004-5311 under project PPQ2003-01326.

JE0602824